Journal of Structural Geology 32 (2010) 1834–1849

Contents lists available at ScienceDirect

Journal of Structural Geology

journal homepage: www.elsevier.com/locate/jsg

Clay smear in normal fault zones – The effect of multilayers and clay cementation in water-saturated model experiments

J. Schmatz [a], [*], P.J. Vrolijk [b], J.L. Urai [a]

[a] *Structural Geology, Tectonics and Geomechanics, Geological Institute, RWTH Aachen University, Lochnerstrasse 4-20, 52056 Aachen, Germany*
[b] *ExxonMobil Upstream Research Co., P.O. Box 2189, Houston, TX, USA*

ARTICLE INFO

Article history:
Received 29 April 2009
Received in revised form
10 December 2009
Accepted 13 December 2009
Available online 4 January 2010

Keywords:
Clay smear
Fault seal
Mechanical layering
Competence contrast
Experimental model

ABSTRACT

We studied the evolution of fault zones in water-saturated model experiments consisting of sand and clay layers above a normal fault dipping 70° in a stiff basal layer. The model is bounded below by a rigid metal basement with a pre-cut 70° fault and above by a metal plate, also with a 70° cut, aligned in the same plane as the basement fault. Quantitative analysis of particle displacements was undertaken with PIV (Particle Image Velocimetry) software. In these models, the structure of initial localized deformation evolves into a kinematically favorable fault zone. This evolution, which produces releasing or restraining relays across the clay layer, has a major role in controlling fault-zone structure. We show that a high competence contrast between sand and clay leads to a more complex fault zone due to the formation of secondary shear zones and segmentation-induced fault lenses. A high competence contrast also promotes a more complex temporal evolution of those shear zones. Weak clay layers are preferentially enriched in fault zones, whereas strong, brittle clay initially fractures and forms clay boudins that rotate in the deforming sand. With progressive deformation these boudins are abraded and transformed into a soft-clay gouge. Thin, weak clays deform continuously over large displacements, and the volume of clay-rich gouge increases as sand mixes into clay at the margins of the shear zone. Thus, we observe a wide range of fault zone and fault gouge evolution by adjusting the mechanical properties of the clay. Further physical insights into fault processes like those reached here may yield predictive models of fault-zone evolution that will transcend empirical methods (e.g., shale-gouge ratio, SGR).

1. Introduction

Fault networks have a major effect on hydromechanical processes in sedimentary basins. We have a basic understanding of the basic physical processes of fault sealing, but the complex geometries and many feedback processes make quantitative prediction difficult. Fault zones have been widely investigated in field studies, experimental models and numerical simulations to better understand their transport and sealing properties (e.g., Weber et al., 1978; Lehner and Pilaar, 1991, 1997; Antonellini et al., 1994; Fulljames et al., 1997; Clausen and Gabrielsen, 2002; James et al., 2004; Egholm et al., 2008; Mair and Abe, 2008; Urai et al., 2008).

Much of the research on faults in sand–clay sequences is focused on predicting the amount of clay incorporated into the fault gouge, commonly called clay smear. Clay smear, a loosely defined term used in hydrocarbon geology, describes the processes in which clay from the wall rock is incorporated in a fault zone (Yielding et al., 1997). In subsurface studies, numerous statistical algorithms are used for clay smear analysis: clay-smear potential, shale-smear factor and shale-gouge ratio (Lindsay et al., 1993; Fristad et al., 1997; Fulljames et al., 1997; Yielding et al., 1997; Yielding, 2002). Most of these methods are based on the assumption that fault gouge consists of a reworked equivalent of the wall rocks offset by a fault (Holland et al., 2006) without the addition or removal of material (van Gent et al., in press). Because this method averages over the lithologic interval offset by the fault, it fails to accurately predict the spatial distribution of clay along the fault plane. In addition, the mechanical properties of the rocks in the wall rock and fault zone are neglected. Clearly, a better understanding of the processes involved during faulting would improve the quality of fault-seal predictions.

When a segmented normal fault cuts heterogeneously layered sequences with competence contrast, (e.g., clay and sand), the fault develops a steeper dip in layers with a higher friction angle and a shallower dip in layers with a lower friction angle (Peacock and Sanderson, 1992). This results in vertically segmented faults with steps at lithologic/competency boundaries (Childs et al., 1996).

---

[*] Corresponding author. Fax: +49 80 92358.
E-mail addresses: j.schmatz@ged.rwth-aachen.de (J. Schmatz), peter.vrolijk@exxonmobil.com (P.J. Vrolijk), j.urai@ged.rwth-aachen.de (J.L. Urai).

0191-8141/$ – see front matter © 2009 Elsevier Ltd. All rights reserved.
doi:10.1016/j.jsg.2009.12.006

Other authors (e.g., Lehner and Pilaar, 1997; Van der Zee et al., 2003) postulated that "clay injection" is able to enrich the fault with clay over the amount expected by lithologic offset. The clay injection mechanism proposed by Lehner and Pilaar (1997) contains two essential elements: (1) a pull-apart structure forms when the fault crosses a clay layer. (2) The clay bed is injected into this pull-apart structure and subsequently sheared to form a thick clay gouge. The injection process requires significantly weaker clay than the surrounding sand layers (Van der Zee et al., 2003). van Gent et al. (in press) describe a fundamentally different process of clay enrichment, which involves the vertical transport of clay along dilatant fractures in brittle carbonates.

Experiments by Sperrevik et al. (2000) and Clausen and Gabrielsen (2002) showed a strong dependency of clay smear on the mechanical properties of the materials. They used a ring-shear apparatus to deform clay and sand layers to high strains at variable normal stresses. They observed pronounced clay smear with increasing stresses and decreasing clay strength. In a preliminary set of experiments of layered sand–clay sequences, Schmatz et al. (2010) varied the clay-layer proportions, clay-layer thickness and spacing, and clay composition; normal faulting created continuous smear in weak, under-consolidated clay; in contrast, a strong, over-consolidated clay first deforms in a brittle mode and then sometimes becomes reworked to form a soft-clay gouge. Here we present the results of water-saturated experiments with the added boundary condition of a strong top layer containing a pre-cut fault in a kinematically favorable orientation to the basement fault, and investigate the effect of different multilayer configurations and clay cementation on the structure of the evolving fault zone.

In experiments with a free top surface, deformation is less localized at the top of the model (Fig. 1). Pilot experiments (Schmatz et al., 2010) show that a top plate and basement fault acting together form two precursor faults: one initiating at the tip of the basement fault, and one at the tip of the fault in the top plate (cf. quadshear, Welch et al., 2009). With progressive deformation they link up across the model to form a kinematically favored zone of deformation.

2. Methods

2.1. Setup

A sandbox was constructed to deform water-saturated, layered ($40 \times 20 \times 20$ cm) (width/height/depth) sand–clay models (Fig. 2). In this series of experiments, the boundary conditions were chosen to simulate a series of weaker layers sandwiched between two strong and stiff layers cut by two co-planar faults dipping 70° (see also Mandl, 2000; Van der Zee, 2002; Ferrill and Morris, 2003; Adam et al., 2005). Water-saturated models allowed the deformation of wet clay and cohesionless sand together in one model (Schmatz et al., 2010). The basement fault moved at 40 mm/h to a maximum offset of 60 mm. The models were run between two glass plates lubricated to minimize edge effects. At this deformation rate, the thick clay layers were sheared under undrained conditions, whereas pore pressures likely remained hydrostatic inside the fine-grained sand. The resulting material properties were characterized by a series of standard geotechnical measurements. Full details of the methods for a free-surface boundary condition are given in Schmatz et al. (2010). Here we summarize the most important aspects and procedures that result from additional boundary conditions and experiment designs.

2.2. Boundary conditions

We used 2 cm thick aluminum ($\rho = 2400$ kg m^{-3}) top plates, pre-cut at the same 70° angle as the basement fault, placed on top of the models and aligned (co-planar) with the basement fault (Fig. 1). The stiff base plate acts as a rigid guide compared to the sediment, and the top plates rotate and move but without bending. Approximately 40 experiments were run using variable clay strengths and number and thicknesses of the clay layers to investigate fault-zone processes. The experiments were recorded with time-lapse photographs (Schmatz et al., 2010) with constant time interval and resolution, and are presented throughout the paper cropped to the same section.

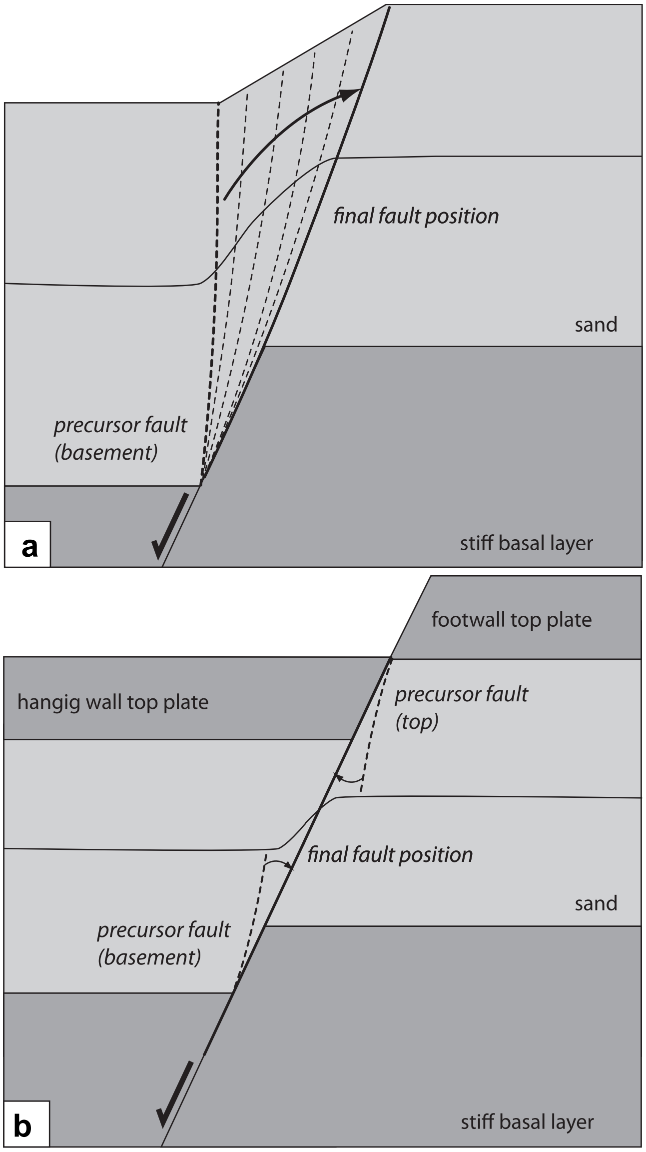

Fig. 1. (a) Sketch showing boundary conditions and fault evolution in an experiment with a free surface. The steep precursor fault is shown with a dashed line. The fault rotates into its kinematically favored position (bold line). Compare to Schmatz et al. (2010). (b) Sketch showing boundary conditions and fault evolution in an experiment with rigid top plates. Two precursor faults develop, initiating at the tip of the faults in the basement and top plates. With progressive deformation, the zone of deformation migrates into the center of the model (bold line).

2.3. Sand

We used the same washed, well-sorted quartz sand with a grain size of 0.1–0.4 mm as in Schmatz et al. (2010), with colored marker horizons. The grain size range results in sand packing classified as medium-dense; thus, the sand yields at a distinct peak shear